

Translating thermal response of triblock copolymer assemblies in dilute solution to macroscopic gelation and phase separation

Zhe Sun,^[a] Ye Tian,^[b] Wendy L. Hom,^[a] Oleg Gang,^{[b],[c],[d]} Surita R. Bhatia,^[a] and Robert B. Grubbs^{*[a]}

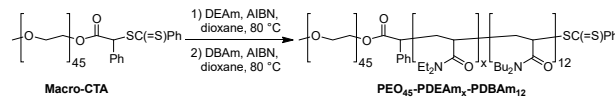
Abstract: The thermal response of semi-dilute solutions (5 w/w%) of two amphiphilic thermoresponsive poly(ethylene oxide)-*b*-poly(*N,N*-diethylacrylamide)-*b*-poly(*N,N*-dibutylacrylamide) (PEO₄₅-PDEAm_x-PDBAm₁₂) triblock copolymers, which differ only in the size of the central responsive block, in water was examined. Aqueous PEO₄₅-PDEAm₄₁-PDBAm₁₂ solutions, which undergo a thermally induced sphere-to-worm transition in dilute solution, were found to reversibly form soft ($G' \approx 10$ Pa) free-standing physical gels after 10 min at 55 °C. PEO₄₅-PDEAm₈₉-PDBAm₁₂ copolymer solutions, which undergo a thermally induced sphere-to-large compound micelle (LCM) transition in dilute solution, underwent phase separation after heating at 55 °C for 10 min due to sedimentation of LCMs. The reversibility of LCM formation was investigated as a non-specific method for removal of a water-soluble dye from aqueous solution. The composition and size of the central responsive block in these polymers dictate the microscopic and macroscopic response of the polymer solutions as well as the rates of transition between assemblies.

Stimulus-responsive polymers have been exploited in applications including biomedicine, sensing, molecular actuation, and separations.^[1] With block copolymers, the introduction of stimuli-responsive blocks^[2] can strongly influence block copolymer self-assembly and can allow triggered transformations between different assemblies.^[3] The precise morphology adopted by a given block copolymer mainly depends on the relative volume fractions of the hydrophilic and hydrophobic blocks and the interfacial energy associated with the block junction,^[3c, 4] so if the degree of hydrophilicity of a given block can be altered in response to external stimuli, the morphology of the polymer aggregates can change significantly. Several examples of thermally responsive polymers that undergo thermally induced

morphological transitions between well-defined structures in dilute solution have been reported.^[5]

For example, poly(ethylene oxide)-*b*-block-poly(*N*-isopropylacrylamide)-*b*-block-poly(isoprene) (PEO-PNIPAm-PI) triblock copolymers in dilute aqueous solution with specific compositions form small spherical micelles at low temperatures that reassemble into large vesicles after heating above the lower critical solution temperature (LCST) for three weeks.^[5a] More rapid transitions have been demonstrated with polymers with lower molecular weight hydrophilic components.^[5d] We have hypothesized that, in addition to molecular weight effects, interchain hydrogen bonding between PNIPAm amide groups after dehydration above the LCST can kinetically trap micelles and slow further rearrangement. As evidence for this hypothesis, poly(ethylene oxide)-*b*-block-poly(ethylene oxide-*stat*-butylene oxide)-*b*-block-poly(isoprene) (PEO-P(EO/BO)-PI) triblock copolymers were found to undergo a sphere-to-vesicle transition upon heating above the P(EO/BO) LCST within several hours.^[5a]

To further probe this hypothesis, we have investigated the dilute solution behavior of poly(ethylene oxide)-*b*-block-poly(*N,N*-diethylacrylamide)-*b*-block-poly(*N,N*-dibutylacrylamide) (PEO-PDEAm-PDBAm) copolymers synthesized by reversible addition-fragmentation chain transfer (RAFT) polymerization (Scheme 1),^[6] in which the stimulus responsive block has an LCST in water similar to that of PNIPAm but cannot form strong interchain hydrogen bonds. In the course of these studies, we have identified two copolymers, PEO₄₅-PDEAm₄₁-PDBAm₁₂ ($M_n = 5.2$ kg/mol; spherical to worm-like micelle) and PEO₄₅-PDEAm₈₉-PDBAm₁₂ ($M_n = 11.3$ kg/mol; spherical to large compound micelle) that undergo rapid transitions from spherical micelles to larger aggregates upon heating (Scheme 1, Table 1). Herein, we describe the solution behavior of these two copolymers in water at higher concentrations (≥ 5.0 w/w%) before and after heating above the PDEAm LCST.



Scheme 1.

Transmission electron microscopy (TEM) and dynamic light scattering (DLS) studies of dilute aqueous PEO₄₅-PDEAm_x-PDBAm₁₂ solutions (0.10 w/w%; Figure 1A, 1C, Figure S3) confirmed that both triblock copolymers form spherical micelles in water at 25 °C due to their large hydrophilic weight fractions ($f \geq 0.75$).^[7] DLS data suggest that PEO₄₅-PDEAm₈₉-PDBAm₁₂ appears to assemble into slightly larger micelles ($D_h = 26$ nm) than

[a] Dr. Z. Sun, Ms. W. L. Hom, Prof. S. R. Bhatia, Prof. R. B. Grubbs
Department of Chemistry
Stony Brook University
Stony Brook, NY, USA 11764-3400
E-mail: robert.grubbs@stonybrook.edu

[b] Dr. Y. Tian, Dr. O. Gang
Center for Functional Nanomaterials
Brookhaven National Laboratory
Upton, NY, USA 11974

[c] Dr. O. Gang
Department of Chemical Engineering
Columbia University
New York, NY, USA 10027

[d] Dr. O. Gang
Department of Applied Physics and Applied Mathematics
Columbia University
New York, NY, USA 10027

PEO₄₅-PDEAm₄₁-PDBAm₁₂ (D_h = 24 nm), most likely resulting from the significantly larger central corona block in PEO₄₅-PDEAm₈₉-PDBAm₁₂ (Figure S3c).

Heating dilute solutions of both polymers (0.2 °C/min, Figure S4) resulted in significant increases in apparent D_h (DLS) above the LCST of the PDEAm blocks (LCST ≈ 41 °C for M_n = 4.7 kg/mol; LCST ≈ 33 °C for M_n = 9.6 kg/mol).^[8] For PEO₄₅-PDEAm₄₁-PDBAm₁₂, D_h began to increase near 45 °C from 24 nm to greater than 150 nm, while for PEO₄₅-PDEAm₈₉-PDBAm₁₂, D_h increased near 35 °C from 26 nm to almost 300 nm. For both polymer solutions, the changes in apparent D_h were reversible over two heating/cooling cycles (Figure S5).

Table 1. Molecular Characteristics of PEO-PDEAm-PDBAm Triblock Copolymers.

Copolymer ^[a]	M_n (kg/mol) ^[a]		D ^[b]	$f_{\text{hydrophilic}}$ ^[c]	
	PDEAm	total		25 °C	55 °C
PEO ₄₅ -PDEAm ₄₁ -PDBAm ₁₂	5.2	9.4	1.29	0.75	0.20
PEO ₄₅ -PDEAm ₈₉ -PDBAm ₁₂	11.3	15.5	1.34	0.84	0.13

[a] M_n values for PDEAm block and triblock copolymer in kg/mol as determined from the polymerization conversions determined by ¹H NMR of crude reaction mixtures and the molecular weight of the PEO-CTA. [b] Dispersity (D) determined by SEC in THF calibrated with PS standards. [c] Hydrophilic weight fraction calculated by the mass of the hydrophilic block or blocks (PEO and PDEAm at 25 °C; PEO at 55 °C) to the total mass of polymer.

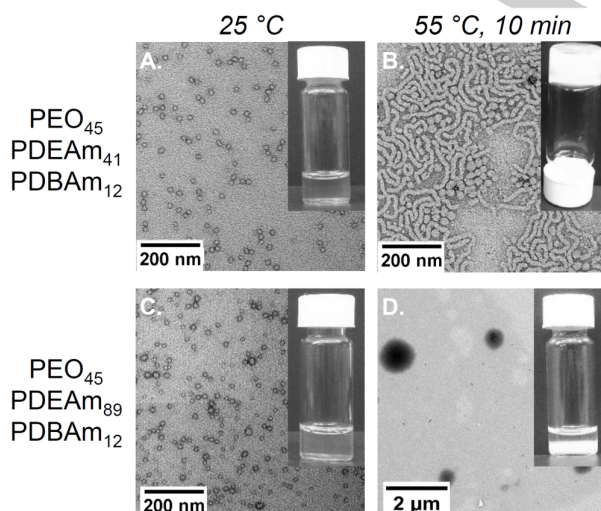


Figure 1. TEM images of 0.1 w/w% aqueous solutions of PEO₄₅-PDEAm₄₁-PDBAm₁₂ (A, B) and PEO₄₅-PDEAm₈₉-PDBAm₁₂ (C, D) at 25 °C and after heating at 55 °C for 10 min. Inset images are photographs of vials of 5.0 w/w% solutions of the indicated polymers at the given temperature. Scale bars (A-C): 200 nm; (D): 2 μm. Color image available in Supporting Information.

TEM images of PEO₄₅-PDEAm₄₁-PDBAm₁₂ samples prepared from 0.1 w/w% solutions after heating at 55 °C for 10 min (Figure 1B), showed the spherical micelles had grown into worm-like micelles. TEM images of PEO₄₅-PDEAm₈₉-PDBAm₁₂ solutions (0.1 w/w%) showed the formation of large polydisperse spheres without any bilayer contrast after heating at 55 °C for 10 min (Figure 1D). These spheres resemble the “large compound micelles” (LCMs) reported previously for amphiphilic block copolymers with very large hydrophobic blocks.^[9] The fast transformation rate from spheres to worms or spheres to LCMs for PEO₄₅-PDEAm₈₉-PDBAm₁₂ block copolymers (~10 min) supports the hypothesis that the absence of strong interchain hydrogen bonding in the thermally responsive block accelerates rearrangement of polymer assemblies.

Amphiphiles with worm-like micelle morphologies can form gels at higher concentrations, even in the absence of specific inter-worm interactions.^[5g, 10] Gelation in these cases has been attributed to topological interactions and requires that worms be sufficiently long and stiff to persist over the time scales probed by rheology.^[10c] The behavior of aqueous solutions of PEO₄₅-PDEAm₄₁-PDBAm₁₂ at higher concentrations (5-10 w/w%) was investigated to determine if the thermally induced sphere-to-worm transition could result in gelation. A transparent aqueous solution of PEO₄₅-PDEAm₄₁-PDBAm₁₂ (5.0 w/w%) was heated at 55 °C. After 10 min the solution formed a soft free-standing physical gel (Figure 1B). Visible degelation occurred within 30-40 s after the sample was removed from the heating bath (Video S1). Repeated heating and cooling experiments indicated that the gelation is completely thermoreversible. In contrast, phase separation was observed in the PEO₄₅-PDEAm₈₉-PDBAm₁₂ aqueous solutions (5.0 w/w %) after heating at 55 °C for 10 min, as the concentrated large compound micelles settled to the bottom of the solution (Figure 1D).

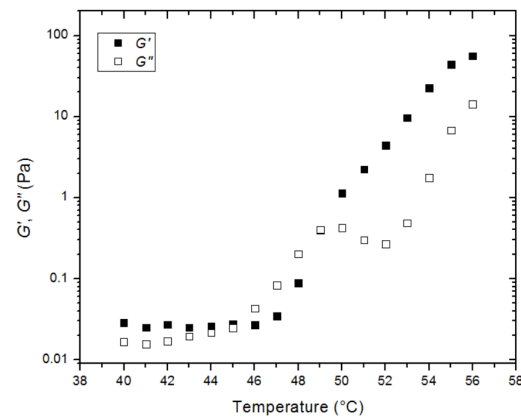


Figure 2. Temperature sweep from 40 °C to 55 °C of 5.0 w/w% PEO₄₅-PDEAm₄₁-PDBAm₁₂ solutions/gels for G' (filled squares) and G'' (open squares) at a fixed frequency of 1.0 Hz and 5.0 % strain.

Oscillatory temperature sweep experiments (Figure 2) confirm gelation: the storage modulus (G') of 5.0 w/w% aqueous PEO₄₅-PDEAm₄₁-PDBAm₁₂ triblock copolymer solutions begins to

exceed the loss modulus (G'') at 49 °C,^[10a] which agrees well with the temperature (45 °C) at which the onset of assembly growth is observed in dilute solutions. Frequency sweeps at 55 °C clearly show a characteristic gel-like response, with G' relatively independent of frequency and greater than G'' over the entire range of measured frequencies (Figure S6).^[10a, 11] This can be contrasted with the results from frequency sweeps taken at 25 °C and 45 °C (Figure S6), in which both G' and G'' show a frequency-dependence characteristic of a viscoelastic liquid. The gel phase is fairly soft, with G' increasing from 10-100 Pa as the polymer concentration was raised from 5.0 to 10.0 w/w% (Figure S7).

The small dip in the value of G'' that can be seen in the temperature sweeps immediately after the gel transition (49–52 °C) (Figure 2), is somewhat curious. This feature appears reproducibly in temperature sweeps of various samples at different concentrations (Figure S7), and likely results from two competing phenomena: (1) the growth of worm-like micelles resulting from the thermally induced change in polymer amphiphilicity, and (2) the decrease in worm-like micelle length and relaxation time that has been seen in surfactant-based worm-like micelles with increasing temperature.^[10c] As the temperature increases, this competition would lead to a complex dependence of the moduli on temperature near the gel transition. Eventually the increasing length of the micelles dominates, and gel formation is favored.

Potential applications of large compound micelles have not been widely explored. The presence of hydrophilic domains within a large excluded phase suggests that the reversible formation of large compound micelles could be of use in the encapsulation and concentration of water-soluble contaminants in water. The encapsulating ability of the large compound micelles formed by PEO₄₅-PDEAm₈₉-PDBAm₁₂ was investigated by dye-encapsulation experiments using the hydrophilic dye rhodamine B (Table S1). An aqueous solution of PEO₄₅-PDEAm₈₉-PDBAm₁₂ (5.0 w/w %) and rhodamine B (~2 ppm) was heated at 55 °C to induce phase separation and the top aqueous layer (~0.4 ppm rhodamine B) was removed. A small amount of 55 °C water added atop the bottom polymer-rich layer remained clear after 10 min at 55 °C with minimal extraction of rhodamine B (~0.08 ppm) from the polymer phase (Figure S8), indicating that rhodamine B was encapsulated inside the large compound micelles. Cooling the bottom layer down to 25 °C resulted in reformation of a transparent micelle solution enriched with rhodamine B (~2.7 ppm) (Figure S9).

In summary, two members of a new class of thermally responsive ABC PEO-PDEAm-PDBAm triblock copolymers synthesized by RAFT polymerization show macroscopic behavior in semidilute solution that reflects the microscopic changes observed in dilute solution: copolymers that undergo a spherical-to-cylindrical micelle transition in dilute solution form gels at higher concentrations, while copolymers that undergo a spherical-to-large-compound micelle transition in dilute solution undergo phase separation at higher concentrations. The fast heating-induced growth rates (within 10 minutes), even faster transitions back to spherical micelles upon cooling (within 1 minute), and reversibility of the transformations support our hypothesis that the absence of strong interchain hydrogen bonding in the central

thermally responsive block facilitates rapid growth of smaller aggregates into larger ones at the macroscopic as well as the microscopic level. Further manipulation of block copolymer composition and monomer functionality should allow the development of control over gelation temperature and rate, as well as the ability of large compound micelles to encapsulate hydrophilic compounds.

Experimental Section

Experimental details are available in the supporting information.

Acknowledgements

This research was supported by the National Science Foundation (R.B.G.: DMR-1105622; S.R.B.: CBET-1335787) and was partially carried out at the Center for Functional Nanomaterials, a U.S. DOE Office of Science Facility, at Brookhaven National Laboratory under Contract No. DE-SC0012704.

Keywords: Block copolymers • Gels • Micelles • Nanostructures • Self-assembly

- [1] a) M. A. Stuart, W. T. Huck, J. Genzer, M. Müller, C. Ober, M. Stamm, G. B. Sukhorukov, I. Szleifer, V. V. Tsukruk, M. Urban, F. Winnik, S. Zauscher, I. Luzinov, S. Minko, *Nat Mater* **2010**, *9*, 101-113; b) M. I. Gibson, R. K. O'Reilly, *Chem. Soc. Rev.* **2013**, *42*, 7204-7213; c) D. Roy, W. L. Brooks, B. S. Sumerlin, *Chem. Soc. Rev.* **2013**, *42*, 7214-7243; d) E. G. Kelley, J. N. L. Albert, M. O. Sullivan, T. H. Epps, *Chem. Soc. Rev.* **2013**, *42*, 7057-7071; e) M. Karimi, A. Ghasemi, P. Sahandi Zangabad, R. Rahighi, S. M. Moosavi Basri, H. Mirshekari, M. Amiri, Z. Shafaei Pishabad, A. Aslani, M. Bozorgomid, D. Ghosh, A. Beyzavi, A. Vaseghi, A. R. Aref, L. Baghani, S. Bahrami, M. R. Hamblin, *Chem. Soc. Rev.* **2016**, *45*, 1457-1501; f) L. Sambe, V. R. de La Rosa, K. Belal, F. Stoffelbach, J. Lyskawa, F. Delattre, M. Bria, G. Cooke, R. Hoogenboom, P. Woisel, *Angew. Chem. Int. Ed. Engl.* **2014**, *53*, 5044-5048; g) A. Yamada, Y. Hiruta, J. Wang, E. Ayano, H. Kanazawa, *Biomacromolecules* **2015**, *16*, 2356-2362; h) S. Uchiyama, N. Kawai, A. P. de Silva, K. Iwai, *J. Am. Chem. Soc.* **2004**, *126*, 3032-3033; i) C. Li, N. Gunari, K. Fischer, A. Janshoff, M. Schmidt, *Angew. Chem. Int. Ed. Engl.* **2004**, *43*, 1101-1104.
- [2] R. B. Grubbs, Z. Sun, *Chem. Soc. Rev.* **2013**, *42*, 7436-7445.
- [3] a) Y. Mai, A. Eisenberg, *Chem. Soc. Rev.* **2012**, *41*, 5969-5985; b) T. H. Epps, R. K. O'Reilly, *Chem. Sci.* **2016**, *7*, 1674-1689; c) A. Blanazs, S. P. Armes, A. J. Ryan, *Macromol. Rapid Commun.* **2009**, *30*, 267-277.
- [4] J. N. Israelachvili, *Intermolecular and Surface Forces Preface to the Third Edition*, **2011**.
- [5] a) Sundararaman, T. Stephan, R. B. Grubbs, *J. Am. Chem. Soc.* **2008**, *130*, 12264-12265; b) D. Roy, J. N. Cambre, B. S. Sumerlin, *Chem. Commun.* **2009**, 2106-2108; c) J. P. Zhao, G. Z. Zhang, S. Pispas, *J. Polym. Sci., Part A: Polym. Chem.* **2009**, *47*, 4099-4110; d) A. O. Moughton, R. K. O'Reilly, *Chem. Commun.* **2010**, *46*, 1091-1093; e) A. E. Smith, X. Xu, S. E. Kirkland-York, D. A. Savin, C. L. McCormick, *Macromolecules* **2010**, *43*, 1210-1217; f) Y. Cai, K. B. Aubrecht, R. B. Grubbs, *J. Am. Chem. Soc.* **2011**, *133*, 1058-1065; g) A. Blanazs, R. Verber, O. O. Mykhaylyk, A. J. Ryan, J. Z. Heath, C. W. Douglas, S. P. Armes, *J. Am. Chem. Soc.* **2012**, *134*, 9741-9748; h) J. Y. Quek, Y. C. Zhu, P. J. Roth, T. P. Davis, A. B. Lowe, *Macromolecules* **2013**, *46*, 7290-7302; i) R. Banerjee, D. Dhara, *Langmuir* **2014**, *30*, 4137-4146; j) M. H. Dan, F. Huo, X. Xiao, Y. Su, W. Q. Zhang, *Macromolecules* **2014**, *47*,

1360-1370; k) K. Wei, L. Su, G. Chen, M. Jiang, *Polymer* **2011**, *52*, 3647-3654.

[6] a) A. Walther, P. E. Millard, A. S. Goldmann, T. M. Lovestead, F. Schacher, C. Barner-Kowollik, A. H. E. Muller, *Macromolecules* **2008**, *41*, 8608-8619; b) Y. T. Li, B. S. Lokitz, C. L. McCormick, *Macromolecules* **2006**, *39*, 81-89.

[7] D. E. Discher, F. Ahmed, *Ann. Rev. Biomed. Eng.* **2006**, *8*, 323-341.

[8] a) R. Freitag, T. Baltes, M. Eggert, *J. Polym. Sci., Part A: Polym. Chem.* **1994**, *32*, 3019-3030; b) D. G. Lessard, M. Ousalem, X. X. Zhu, A. Eisenberg, P. J. Carreau, *J. Polym. Sci., Part B: Polym. Phys.* **2003**, *41*, 1627-1637.

[9] a) L. Zhang, A. Eisenberg, *Science* **1995**, *268*, 1728-1731; b) L. F. Zhang, A. Eisenberg, *J. Am. Chem. Soc.* **1996**, *118*, 3168-3181; c) N. J. Warren, O. O. Mykhaylyk, A. J. Ryan, M. Williams, T. Doussineau, P. Dugourd, R. Antoine, G. Portale, S. P. Armes, *J. Am. Chem. Soc.* **2015**, *137*, 1929-1937.

[10] a) Z. Chu, C. A. Dreiss, Y. Feng, *Chem. Soc. Rev.* **2013**, *42*, 7174-7203; b) R. Kumar, G. C. Kalur, L. Ziserman, D. Danino, S. R. Raghavan, *Langmuir* **2007**, *23*, 12849-12856; c) S. R. Raghavan, J. F. Douglas, *Soft Matter* **2012**, *8*, 8539-8546.

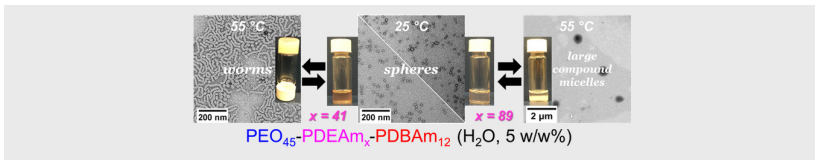
[11] S. K. Ahn, R. M. Kasi, S. C. Kim, N. Sharma, Y. X. Zhou, *Soft Matter* **2008**, *4*, 1151-1157.

COMMUNICATION

Entry for the Table of Contents (Please choose one layout)

Layout 2:

COMMUNICATION



Zhe Sun, Ye Tian, Wendy L. Hom, Oleg Gang, Surita R. Bhatia, and Robert B. Grubbs*

Page No. – Page No.

Translating thermal response of triblock copolymer assemblies in dilute solution to macroscopic gelation and phase separation

Midblock management. The size of the central responsive block of an amphiphilic triblock copolymer determines structural changes upon heating and affects whether gelation or phase separation occurs in semi-dilute solution.

Translating thermal response of triblock copolymer assemblies in dilute solution to macroscopic gelation and phase separation

Zhe Sun,[†] Ye Tian,[‡] Wendy L. Hom,[†] Oleg Gang,[‡] Surita R. Bhatia,[†] and Robert B. Grubbs*,[†]

[†]Department of Chemistry, Stony Brook University, Stony Brook, New York 11794-3400, United States.

[‡]Center for Functional Nanomaterials, Brookhaven National Laboratory, Upton, New York 11973, United States

Supporting Information

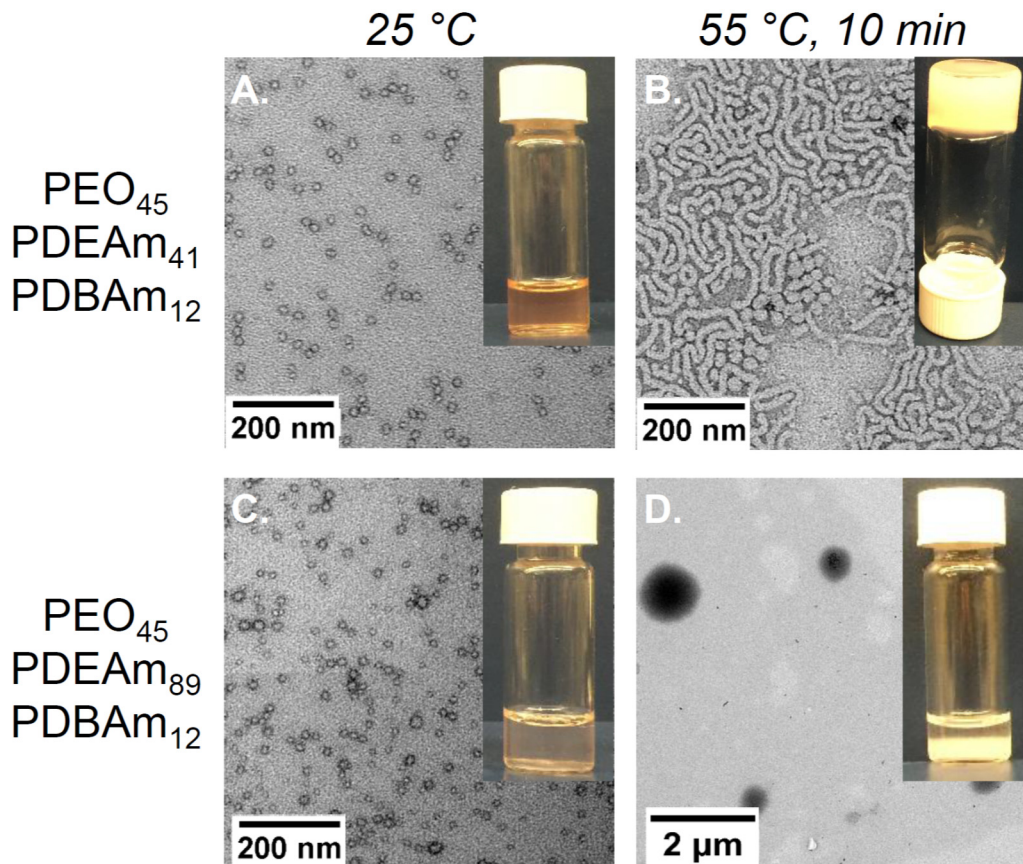


Figure 1 (color). TEM images of 0.1 w/w% aqueous solutions of $\text{PEO}_{45}\text{-PDEAm}_{41}\text{-PDBAm}_{12}$ (A, B) and $\text{PEO}_{45}\text{-PDEAm}_{89}\text{-PDBAm}_{12}$ (C, D) at 25 °C and after heating at 55 °C for 10 min. Inset images are photographs of vials of 5.0 w/w% solutions of the indicated polymers at the given temperature. Scale bars (A-C): 200 nm; (D): 2 μm.

Materials

2,2-Azobis(isobutyronitrile) (AIBN, 98%, Sigma-Aldrich) was recrystallized twice from methanol. Carbon disulfide (99.9+%, EMD), triethylamine (99.9+%, EMD), 1,4-dioxane (99.9+%, EMD), tetrahydrofuran (99.9%, EMD), and dichloromethane (99.8%, EMD) were used after storage on molecular sieves (4Å, 1-2 mm beads, Alfa Aesar) overnight. Poly(ethylene oxide) methyl ester (PEO) (Sigma-Aldrich, $M_n = 2000$ g/mol, $D = 1.02$) was freeze-dried from benzene before use. All other chemicals and solvents were purchased from Fisher or Sigma-Aldrich at the highest available purity and used as received. Distilled deionized water was used to prepare polymer solutions.

Characterization

Nuclear Magnetic Resonance Spectroscopy (NMR). ^1H NMR spectroscopy was carried out on a 300 MHz Varian Gemini 2300 spectrometer using CDCl_3 as solvent. Chemical shifts were referenced to the residual proton peak of CDCl_3 (7.26 ppm).

Gel Permeation Chromatography (GPC). GPC was performed at 40 °C using THF (HPLC grade, J.T. Baker) eluent at a flow rate of 1.0 mL/minute at 40 °C. The apparatus consisted of a K-501 pump (Knauer), a K-3800 Basic Autosampler (Marathon), two PLgel 5 μm Mixed-D columns (300 X 7.5 mm, rated for polymers between 200-400,000 g/mol, Polymer Laboratories), and a PL-ELS 1000 Evaporative Light Scattering Detector (Polymer Laboratories). A PL Datastream unit (Polymer Laboratories) was used to acquire data, which was analyzed based on narrow polydispersity polystyrene standards in the molecular weight range of 580-400,000 g/mol (EasiCal PS-2, Polymer Laboratories).

Dynamic Light Scattering (DLS). Intensity-average hydrodynamic diameters of the dispersions (0.10 w/w %) in disposable cuvettes were obtained by DLS using a Malvern Zetasizer NanoZS instrument, which was equipped with a 633 nm laser source and a backscattering detector. All data were averaged over three consecutive runs. Temperature-dependent DLS studies were performed at 0.2 °C/min heating rate.

Transmission Electron Microscopy (TEM). PEO-PDEAm-PDBAm polymers were dissolved in water at 25 °C to generate 0.10 w/w % solutions. Copper grids (400 mesh, Ted Pella product #01822) were plasma glow-discharged for 60 s to create a hydrophilic surface. Individual polymer solution samples (0.10 w/w %, 5 μL) were placed onto the freshly glow-discharged grids by pipette and then blotted with filter paper after 2-3 min to remove excess solution. To stain the aggregates, uranyl acetate (0.20 w/v %) solutions (5 μL) were placed on the sample-loaded grid by pipet. After 10 s excess stain solution was removed by blotting with filter paper and the grid was left to air-dry. For TEM sample preparation at higher temperature, the grid was immersed for 2-3 min in a polymer solution heated at 55 °C on a hot plate and then stained as described above, and excess solution was removed immediately via blotting after 10 s. The grids were observed by TEM with a JEOL-1400 electron microscope at 120 kV.

Rheology. All rheology studies were performed in oscillatory shear mode on either a TA Instruments AR-G2 rheometer or a TA Instruments DHR-II rheometer, using a 40-mm aluminum parallel plate geometry and a Peltier plate for temperature control. All oscillatory tests were performed within the linear viscoelastic region determined from strain amplitude sweeps at 55 °C and a frequency of 10.0 Hz. Frequency sweeps at a fixed strain of 5% strain were performed at 55 °C, 45 °C, and 25 °C to determine G' and G'' . Temperature sweeps were performed at a fixed strain of 5% and angular frequency of 1.0 Hz, with a heating rate of 1 °C/min and a 2 minute equilibration time at each temperature before measurement.

Synthetic Procedures

Esterification of PEO₄₅ with α -bromophenylacetic acid (PEO₄₅-bromoester)¹

Poly(ethylene oxide) methyl ester (MeOPEG₄₅) (6.00 g, 3.00 mmol, $M_n = 2.0$ kg/mol) was dissolved in dichloromethane (40 mL). To this solution, α -bromophenylacetic acid (1.29 g, 6.00 mmol), DMAP (49 mg, 0.40 mmol), and dicyclohexylcarbodiimide (2.07 g, 10.0 mmol) were added at room temperature. The reaction mixture was then stirred at room temperature for 24 h under nitrogen. After filtration, the solution was precipitated into hexanes (400 mL). The crude precipitate was isolated by filtration, dissolved in THF (30 mL), precipitated into cold hexanes (500 mL), filtered and dried under vacuum to afford end-functionalized PEO₄₅-bromoester (5.05 g, 80% after 2 precipitations). ¹H NMR (CDCl₃, 300 MHz): 3.36 (3H, s, O-CH₃), 3.55-3.92 (4H per repeating unit, s, CH₂-CH₂-O), 5.39 (1H, s, CHCl), 7.36-7.55 (5H, m, Ar-H).

Synthesis of PEO₄₅ Macro-CTA¹

Carbon disulfide (0.40 mL, 6.60 mmol) was added dropwise to a solution of phenylmagnesium chloride (1.20 mL of a 3.0 M solution in diethyl ether, 3.60 mmol) in dry tetrahydrofuran (10 mL) under nitrogen. The reaction mixture was stirred for 30 min under nitrogen at room temperature, resulting in a dark-red solution. This solution was added to a solution of functionalized PEO₄₅-bromoester (4.00 g, 1.80 mmol) in dry tetrahydrofuran (40 mL), and the reaction mixture was heated at reflux under nitrogen for 24 h. The solution was then filtered and precipitated into hexanes (500 mL) to yield the PEO-RAFT Macro-CTA, **2**, as a pink solid. The crude product was further purified by a second precipitation into hexanes (500 mL) from tetrahydrofuran (30 mL), filtered and dried under vacuum (3.07 g, 75% after 2 precipitations).

¹H NMR (CDCl₃, 300 MHz): 3.33 (s, O-CH₃), 3.53-3.94 (s, CH₂-CH₂-O), 5.65 (1H, s, -S(Ph)CH-CO₂Me), 7.20-7.50 (8H, m, Ar-H), 7.93-8.00 (2H, d, -S(S=C)Ar-H, *ortho*-).

Synthesis of *N,N*-diethylacrylamide (DEAm)²

Diethylamine (4.10 mL, 39.3 mmol) and triethylamine (5.50 mL, 39.5 mmol) were dissolved in dichloromethane (100 mL). The solution was cooled to 0 °C and a solution of acryloyl chloride (3.32 mL, 39.2 mmol) in dichloromethane (20 mL) was added dropwise over 1 h. The reaction mixture was stirred under nitrogen at 0 °C for 1 h and allowed to warm to room temperature over 1 h. The reaction mixture was then washed with saturated sodium bicarbonate solution (2 × 50 mL) and saturated sodium chloride solution (2 × 50 mL). The organic fraction was dried over anhydrous magnesium sulfate, filtered, and concentrated under reduced pressure. The product was dissolved in ethyl acetate (30 mL) and was washed with saturated sodium bicarbonate solution (2 × 50 mL) and saturated sodium chloride solution (2 × 50 mL). Drying over anhydrous magnesium sulfate, followed by filtration and concentration under reduced pressure, yielded an oil that was distilled to yield 2.25 g (45%) of *N,N*-diethylacrylamide (b.p. = 58-59 °C at 0.6 Torr).

¹H NMR (300 MHz, CDCl₃): δ 1.16 (m, 6H, -CH₃), 3.36 (m, 2H, -N(Et)CH₂-), 3.42 (m, 2H, -N(CH₂-)Et), 5.64 (dd, 1H, cis δ =CHH, J = 10.3 and 2.0 Hz), 6.32 (dd, 1H, trans δ =CHH, J = 16.7 and 2.0 Hz), 6.53 (dd, 1H, =CH₂, J = 16.7 and 10.3 Hz).

Synthesis of *N,N*-dibutylacrylamide (DBAm)²

Dibutylamine (6.70 mL, 39.3 mmol) and triethylamine (5.50 mL, 39.5 mmol) were dissolved in dichloromethane (100 mL). The resulting solution was cooled to 0 °C, and a solution of acryloyl chloride (3.32 mL, 39.2 mmol) in dichloromethane (20 mL) was added dropwise over 1 h at 0 °C. The reaction mixture was stirred under nitrogen at 0 °C for 1 h and at room temperature for 1 h. The solution was then washed with saturated sodium bicarbonate solution (2 × 50 mL) and saturated sodium chloride solution (2 × 50 mL). It was then dried over anhydrous magnesium sulfate, filtered, and concentrated under reduced pressure. The product was dissolved in ethyl acetate (30 mL) and was washed with saturated sodium bicarbonate solution (2 × 50 mL) and saturated sodium chloride solution (2 × 50 mL). Drying over anhydrous magnesium sulfate, followed by filtration and concentration under reduced pressure, yielded an oil that was distilled to yield 4.30 g (40%) of *N,N*-dibutylacrylamide (bp = 95-96 °C at 0.6 Torr).

¹H NMR (300 MHz, CDCl₃): δ 1.16 (m, 6H, butyl -CH₃), 1.36 (m, 4H, butyl -CH₂CH₃), 1.54 (m, 4H, butyl -CH₂CH₂CH₃), 3.36 (m, 2H, -N(CH₂-)Bu), 3.42 (m, 2H, -N(Bu)CH₂-), 5.64 (dd, 1H, cis δ =CHH, J = 10.3 and 2.0 Hz), 6.32 (dd, 1H, trans δ =CHH, J = 16.7 and 2.0 Hz), 6.53 (dd, 1H, =CH₂, J = 16.7 and 10.3 Hz)

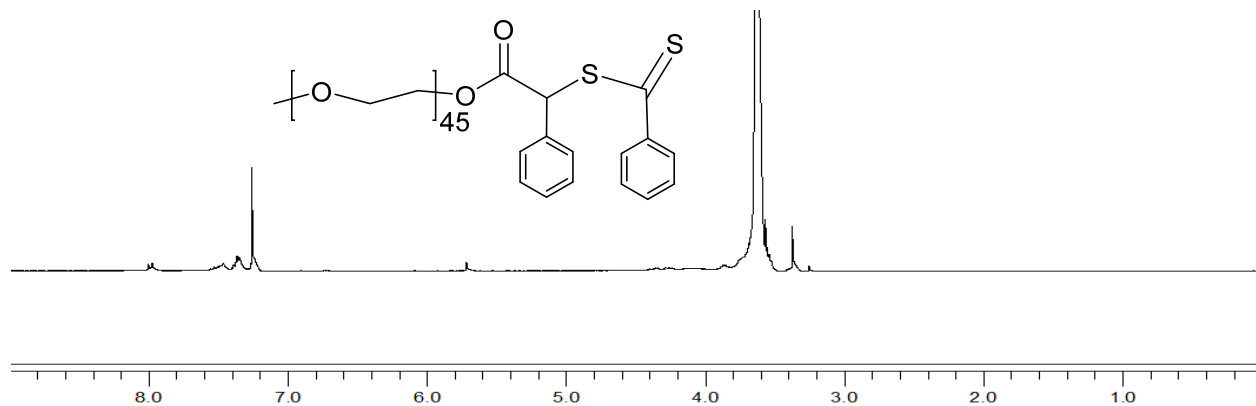
Synthesis of PEO₄₅-PDEAm₄₁ diblock copolymers³

In a typical protocol for the synthesis of PEO₄₅-PDEAm₄₁, DEAm (1.20 g, 9.50 mmol), PEO-CTA (0.46 g, 0.20 mmol), and AIBN (0.004 g, 0.024 mmol) were added along with 1,4-dioxane (1 mL) to a Schlenk flask. The Schlenk flask was degassed via three freeze-pump-thaw cycles, backfilled with nitrogen and

then placed in a preheated oil bath at 80 °C. The polymerization was halted after 24 h by cooling under liquid nitrogen followed by exposure to air. The viscous reaction mixture was dissolved in dichloromethane (5 mL) and precipitated into cold hexanes (200 mL) to give the diblock copolymer as a pink solid. (Yield: 75%, 1.25 g, Conversion = 86% calculated by comparison of residual monomer vinyl peaks in the ^1H NMR spectrum of the crude reaction mixture, $M_n = 7.5$ kg/mol calculated from the ^1H NMR spectrum of the pure diblock, $D = 1.30$). ^1H NMR (CDCl_3 , 300 MHz): 0.8-1.2 (br m, 6H per DEAm repeating unit, $-\text{CH}_3$), 1.4-2.0 (br m, acrylamide backbone), 2.2-2.8 (br m, acrylamide backbone), 2.8-3.5 (br m, backbone/ $-\text{NCH}_2-$), 3.33 (s, 3H, $\text{O}-\text{CH}_3$), 3.5-3.8 (br, $\text{CH}_2-\text{CH}_2-\text{O}$), 7.1-7.4 (br m, Ar-H), 7.8-8.0 (2H, d, $-\text{S}(\text{S}=\text{C})\text{Ar}-\text{H}$, *ortho*-).

Synthesis of PEO₄₅-PDEAm₄₁-PDBAm₁₂ triblock copolymers³

A typical protocol for the synthesis of PEO₄₅-PDEAm₄₁-PDBAm₁₂ is as follows: DBAm (0.11 g, 0.60 mmol), PEO₄₅-PDEAm₄₁ (0.38 g, 0.05 mmol), and AIBN (0.001 g, 0.006 mmol) were added along with 1,4-dioxane (1 mL) to a Schlenk flask. The Schlenk flask was degassed via three freeze-pump-thaw cycles, backfilled with nitrogen and then placed in a preheated oil bath at 80 °C. The reaction solution was stirred 40 h to ensure complete DBAm monomer conversion (>99%) and the polymerization was halted by cooling the reaction vessel in liquid nitrogen followed by exposure of the polymerization solution to air. The viscous reaction mixture was dissolved in dichloromethane (3 mL) and precipitated into cold hexane (100 mL) to give the triblock copolymer as a pink solid. (Yield: 82%, 0.40 g, Conversion > 99% determined by disappearance of monomer *N,N*-dibutylacrylamide vinyl peaks in the ¹H NMR of crude reaction mixture, $M_n = 9.8$ kg/mol calculated by conversion, $D = 1.29$). ¹H NMR (CDCl₃, 300 MHz): 0.7-0.9 (br m, 6H per DBAm repeating unit, butyl -CH₃), 0.8-1.2 (br m, 6H per DEAm repeating unit, -CH₃), 1.1-1.5 (br m, DBAm -CH₂-), 1.4-2.0 (br m, acrylamide backbone), 2.2-2.8 (br m, acrylamide backbone), 2.8-3.5 (br m, backbone/-NCH₂-), 3.33 (s, 3H, O-CH₃), 3.5-3.8 (br, CH₂-CH₂-O).



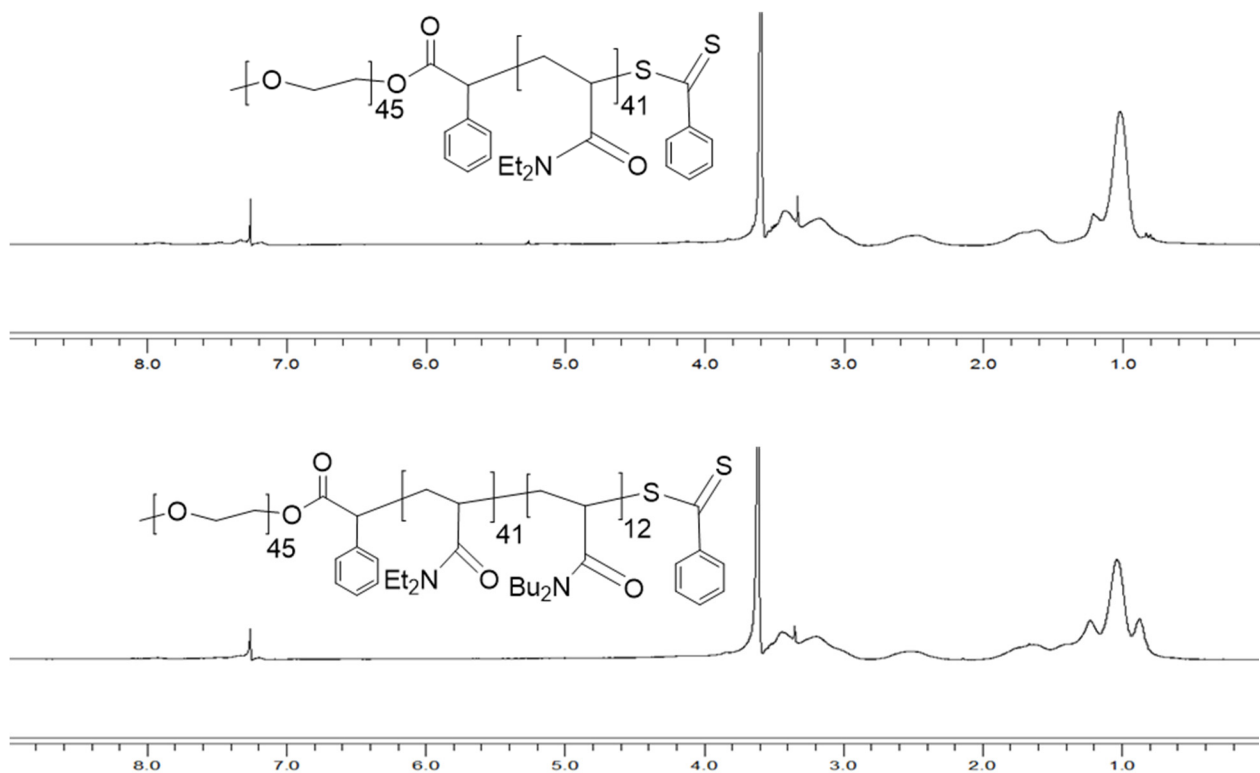
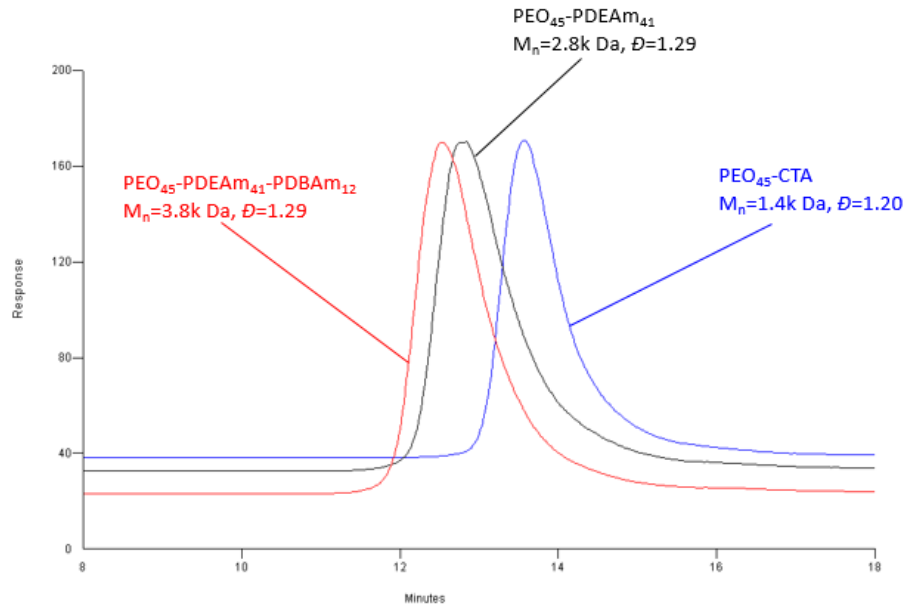


Figure S1. ^1H NMR spectra of PEO₄₅ macro-CTA (top), PEO₄₅-PDEAm₄₁ diblock (middle) and PEO₄₅-PDEAm₄₁-PDBAm₁₂ triblock copolymers (bottom)

(a)



(b)

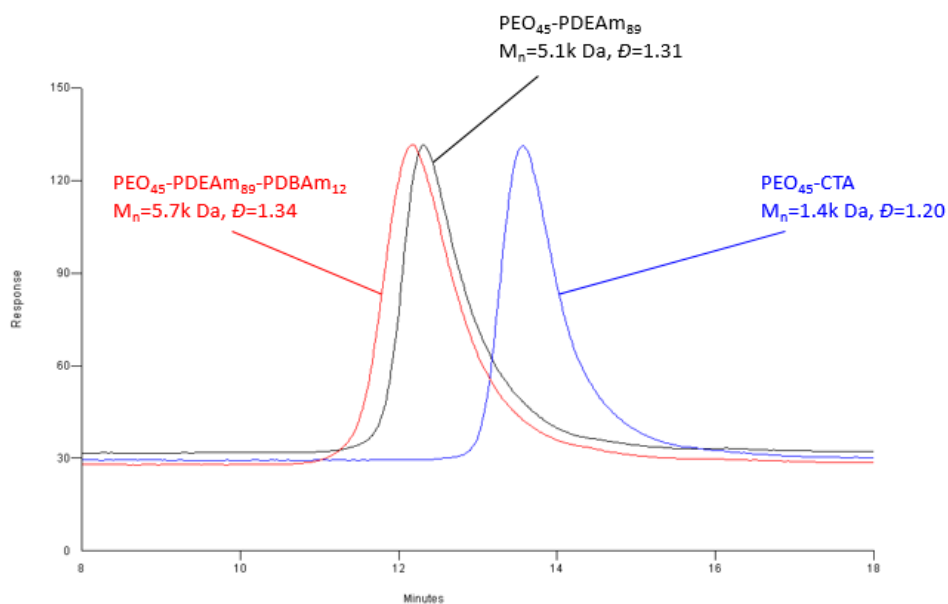


Figure S2. Gel permeation chromatographs obtained in THF for (a) PEO_{45} macro-CTA and the corresponding $\text{PEO}_{45}\text{-PDEAm}_{41}$ diblock copolymer and $\text{PEO}_{45}\text{-PDEAm}_{41}\text{-PDBAm}_{12}$ triblock copolymer and (b) PEO_{45} macro-CTA and corresponding $\text{PEO}_{45}\text{-PDEAm}_{89}$ diblock copolymer and $\text{PEO}_{45}\text{-PDEAm}_{89}\text{-PDBAm}_{12}$ triblock copolymer.

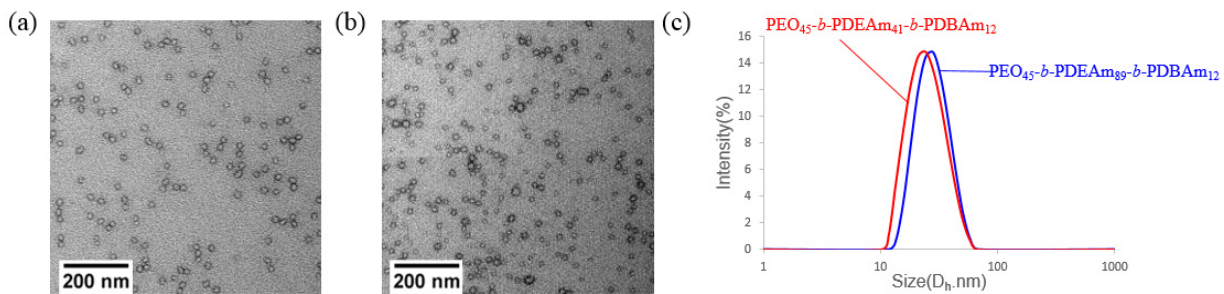


Figure S3. TEM images of the final assembly morphologies in water (0.1 w/w %, stained by uranyl acetate) at 25 °C: (a) PEO₄₅-PDEAm₄₁-PDBAm₁₂ (b) PEO₄₅-PDEAm₈₉-PDBAm₁₂. (c) Normalized DLS particle size distributions (intensity vs mean hydrodynamic diameter, D_h) at 25 °C obtained for PEO₄₅-PDEAm₄₁-PDBAm₁₂ ($D_h = 24$ nm, red) and PEO₄₅-PDEAm₈₉-PDBAm₁₂ ($D_h = 26$ nm, blue)

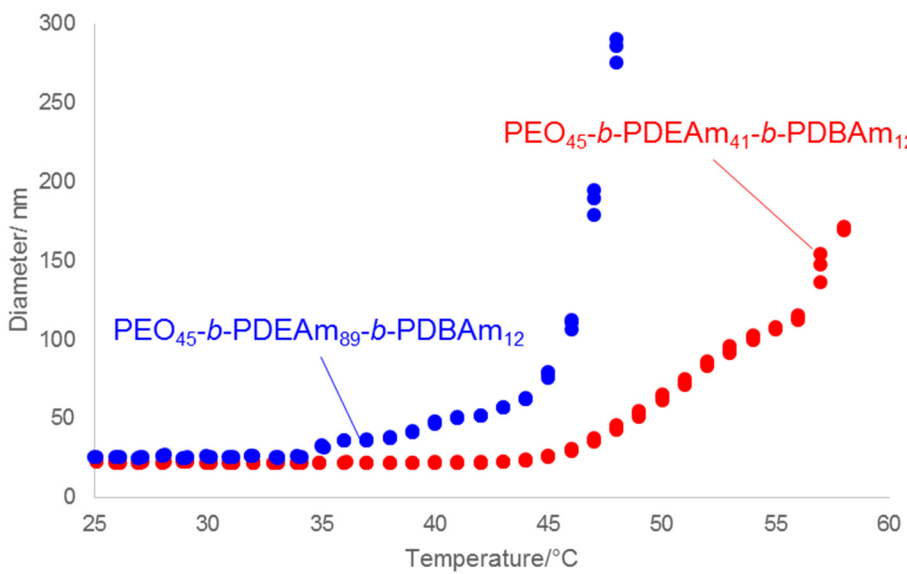


Figure S4. Temperature-dependent intensity-average diameters determined by DLS for 0.1 w/w% aqueous solutions of PEO₄₅-PDEAm₄₁-PDBAm₁₂ (red) and PEO₄₅-PDEAm₈₉-PDBAm₁₂ (blue). Heating rate (0.2 °C/min). Three measurements were taken at each temperature.

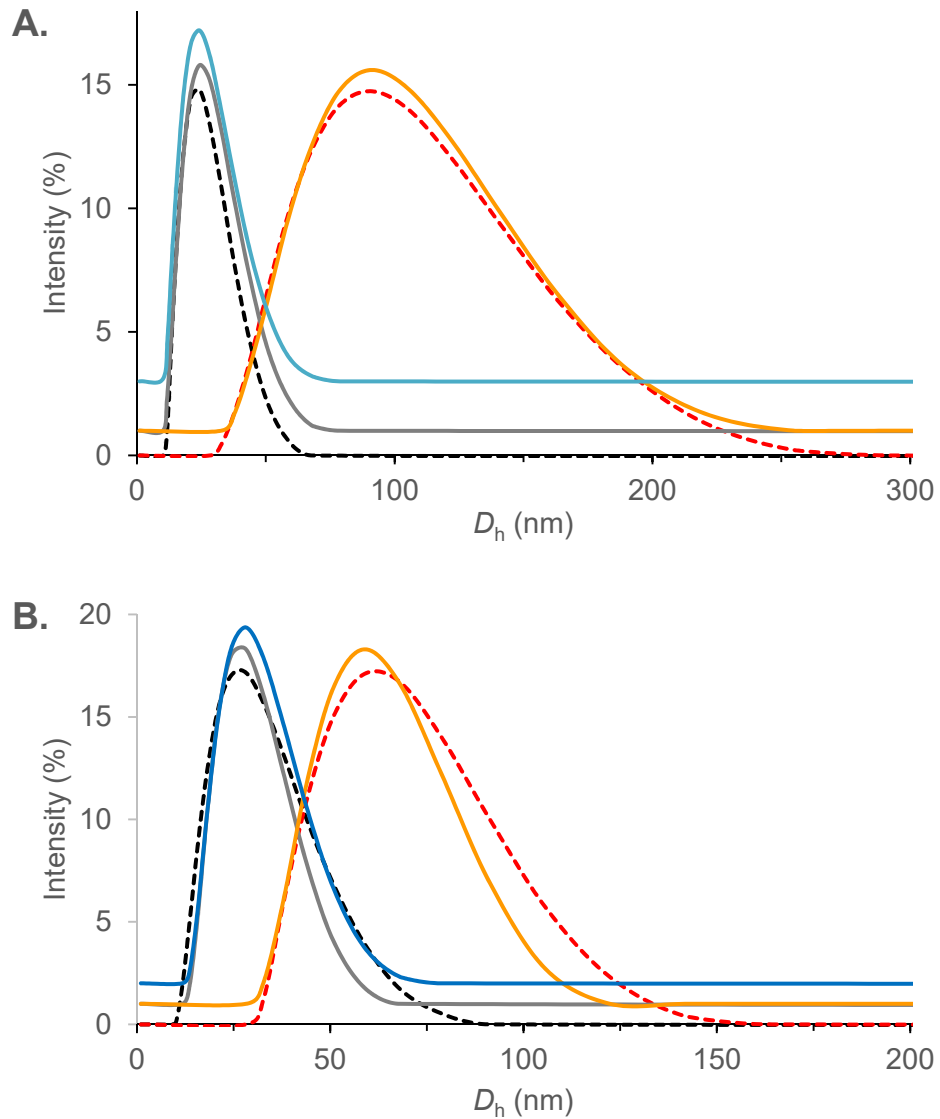


Figure S5. DLS size distributions over two heating/cooling cycles of 0.1 wt% solutions of (A) PEO₄₅-PDEAm₄₁-PDBAm₁₂ at 25 °C prior to first heating (black dashed line, $D_h = 23.9$ nm), after heating at 55 °C for 10 min (red dashed line, $D_h = 81.9$ nm), after first cooling back to 25 °C (grey line, $D_h = 25.9$ nm), after second heating at 55 °C for 10 min (orange line, $D_h = 82.7$ nm), and after second cooling (blue line, $D_h = 24.5$ nm); and (B) PEO₄₅-PDEAm₈₉-PDBAm₁₂ at 25 °C prior to first heating (black dashed line, $D_h = 26.2$ nm), after heating at 55 °C for 10 min (red dashed line, $D_h = 60.5$ nm), after first cooling back to 25 °C (grey line, $D_h = 26.2$ nm), after second heating at 55 °C for 10 min (orange line, $D_h = 57.7$ nm), and after second cooling (blue line, $D_h = 27.8$ nm). The apparent D_h values for PEO₄₅-PDEAm₈₉-PDBAm₁₂ solutions at 55 °C were not consistent with the sizes of the large compound micelles ($d > 300$ nm) observed by TEM and in DLS heating studies. It is possible that large compound micelles settle to the bottom of the DLS cuvette during the 10 min heating period, which leads to unreliable values for D_h of the large compound micelles.

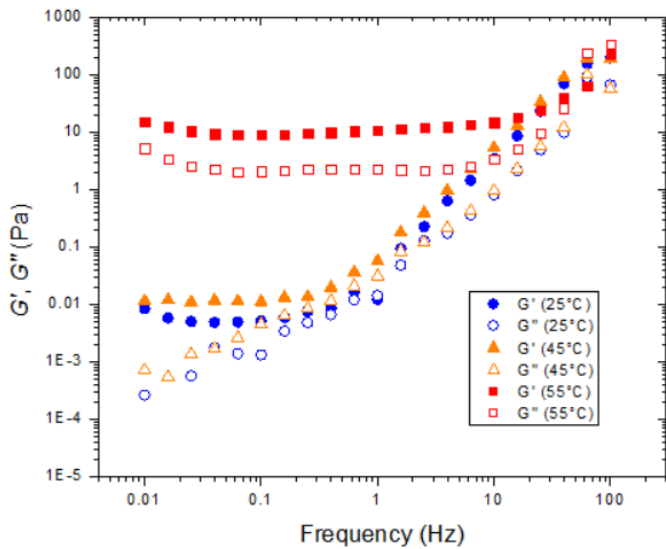


Figure S6. Frequency sweeps of PEO₄₅-PDEAm₄₁-PDBAm₁₂ 5.0 w/w% worm gels at 25 °C, 45 °C and 55 °C at an applied strain of 5.0 %.

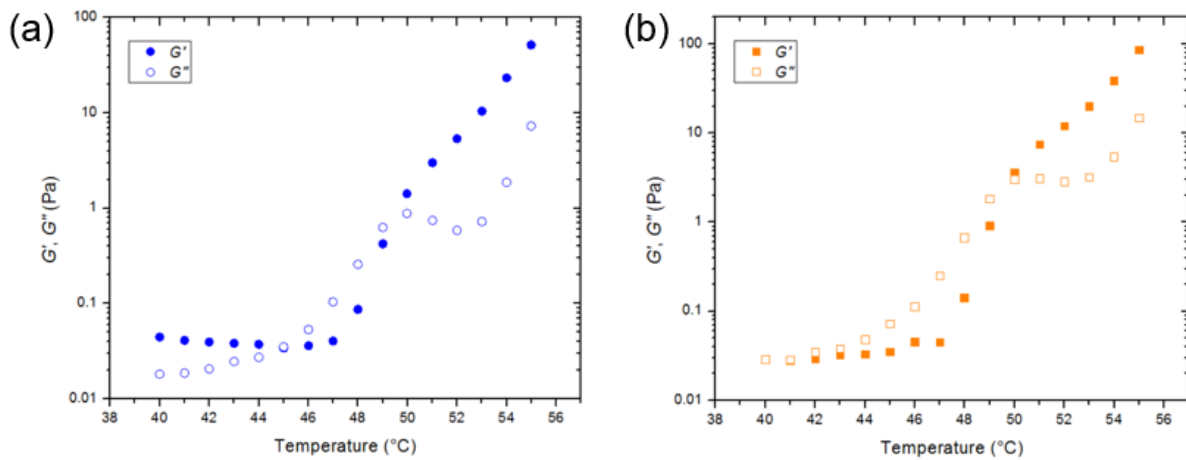


Figure S7. Temperature sweeps of PEO₄₅-PDEAm₄₁-PDBAm₁₂ for G' and G'' from 40 °C to 55 °C at 1.0 Hz and 5.0 % strain: (a) 7.5 w/w% (b) 10.0 w/w%.

Encapsulation of rhodamine B in the large compound micelles of PEO₄₅-PDEAm₈₉-PDBAm₁₂

Rhodamine B (1 mg, 2.4 μ mol) was dissolved in water in a 100 mL volumetric flask to prepare a 0.01 g/L stock solution. 10 mL of the stock solution was then pipetted into a 50 mL volumetric flask and diluted to 50 mL with water for a final concentration of 2.0 mg/L (2 ppm). PEO₄₅-PDEAm₈₉-PDBAm₁₂ triblock copolymer (100 mg, 6.4 μ mol) was dissolved in 1.9 mL of the 2 ppm rhodamine B solution in a 4 mL vial. The resulting solution was stirred at 25 °C for 1 h, at which time the first absorption reading (“original solution”) was taken. The solution was then heated to 55 °C for 15 min to induce phase separation and the top aqueous layer (“top layer after initial heating”) was removed and analyzed for rhodamine B content.⁴ An aliquot of 55 °C water was carefully added atop the polymer phase, and then removed and analyzed for rhodamine B content after 10 min (“second aqueous layer”). The remaining polymer layer was cooled to 25 °C and analyzed for rhodamine B (“final polymer layer”). Rhodamine B concentrations were estimated relative to the initial solution concentration (1.9 ppm) by comparing the ratio of sample absorbance values at 557 nm (A_{557}) to the value for the original solution by UV-vis spectroscopy ($\lambda_{\text{max}} = 557$ nm).

Table S1. Estimated rhodamine B concentrations in large compound micelle encapsulation experiments as measured by absorption spectroscopy.

	A_{557}	Estimated rhodamine B concentration (ppm)
Original solution	0.306	1.9
Top layer after initial heating	0.059	0.37
Second aqueous layer	0.013	0.081
Final polymer layer	0.432	2.7

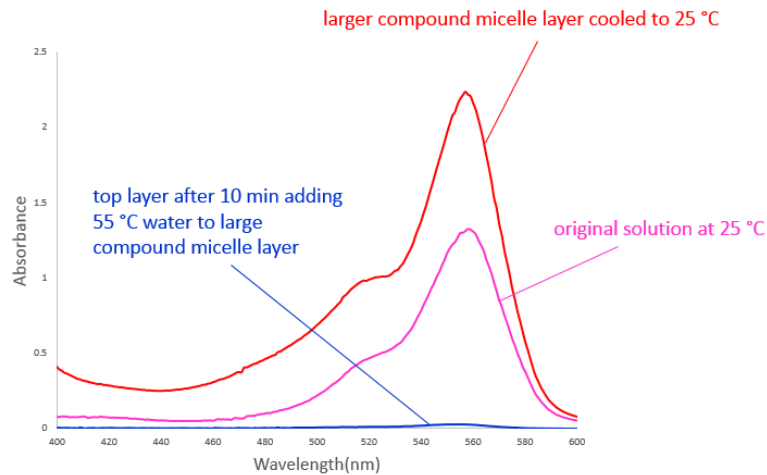


Figure S8. UV-vis spectra of a $\text{PEO}_{45}\text{-PDEAm}_{41}\text{-PDBAm}_{12}$ aqueous solution (initial polymer concentration = 5.0 w/w%) with rhodamine B (initial concentration 0.01 w/w% = 100 ppm).

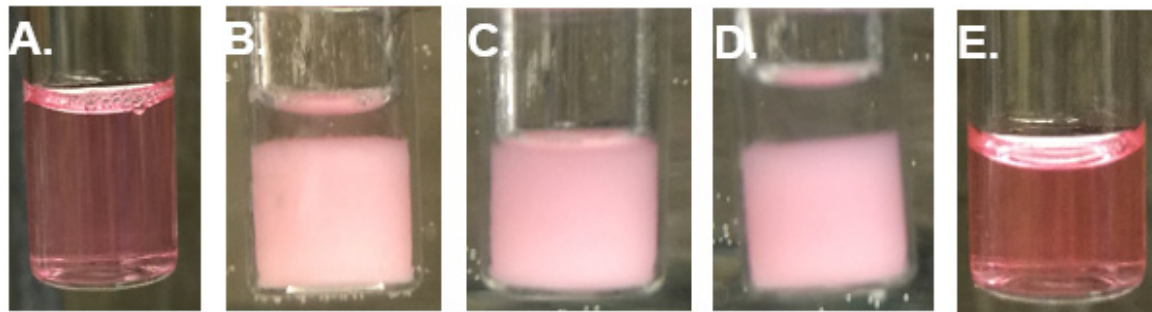


Figure S9. Encapsulation of rhodamine B (2 ppm) with $\text{PEO}_{45}\text{-b-PDEAm}_{89}\text{-b-PDBAm}_{12}$ (5.0 w/w %) solution. A. Initial solution at 25 °C; B. Solution after heating to 55 °C; C. Polymer-rich bottom phase at 55 °C; D. New water layer atop polymer-rich phase at 55 °C; E. Polymer-rich phase after cooling to 25 °C.

Video S1. Video of hydrogel formation and dissolution with a 5.0 w/w% $\text{PEO}_{45}\text{-PDEAm}_{41}\text{-PDBAm}_{12}$ aqueous solution upon heating at 55 °C for 10 min.

References

1. Walther, A.; Millard, P. E.; Goldmann, A. S.; Lovestead, T. M.; Schacher, F.; Barner-Kowollik, C.; Muller, A. H. E., Bis-Hydrophilic Block Terpolymers via RAFT Polymerization: Toward Dynamic Micelles with Tunable Corona Properties. *Macromolecules* **2008**, *41*, 8608-8619. doi: 10.1021/ma801215q.
2. Bergbreiter, D. E.; Aviles-Ramos, N. A.; Ortiz-Acosta, D., A combinatorial approach to studying the effects of N-alkyl groups on poly(N-alkyl and N,N-dialkylacrylamide) solubility. *J. Comb. Chem.* **2007**, *9*, 609-17. doi: 10.1021/cc070016m.

3. Li, Y. T.; Lokitz, B. S.; McCormick, C. L., RA FT synthesis of a thermally responsive ABC triblock copolymer incorporating N-acryloxy succinimide for facile in situ formation of shell cross-linked micelles in aqueous media. *Macromolecules* **2006**, *39*, 81-89. doi: 10.1021/ma052116r.
4. Banerjee, R.; Dhara, D., Functional Group-Dependent Self-Assembled Nanostructures from Thermo-Responsive Triblock Copolymers. *Langmuir* **2014**, *30*, 4137-4146. doi: 10.1021/la500213h.